Journal of Solid Mechanics and Materials Engineering

Vol.4, No.3, 2010

Analysis Method of Friction Torque and Weld Interface Temperature during Friction Process of Steel Friction Welding*

Masaaki KIMURA**, Haruo INOUE***, Masahiro KUSAKA**, Koichi KAIZU** and Akiyoshi FUJI†

** Department of Mechanical and System Engineering, University of Hyogo
2167 Shosha, Himeji, Hyogo, Japan
E-mail: mkimura@eng.u-hyogo.ac.jp

*** Graduate student, University of Hyogo
2167 Shosha, Himeji, Hyogo, Japan

† Department of Mechanical Engineering, National University Corporation-Kitami Institute of Technology
165 Koen-cho, Kitami, Hokkaido, Japan

Abstract

This paper describes an analysis method of the friction torque and weld interface temperature during the friction process for steel friction welding. The joining mechanism model of the friction welding for the wear and seizure stages was constructed from the actual joining phenomena that were obtained by the experiment. The non-steady two-dimensional heat transfer analysis for the friction process was carried out by calculation with FEM code ANSYS. The contact pressure, heat generation quantity, and friction torque during the wear stage were calculated using the coefficient of friction, which was considered as the constant value. The thermal stress was included in the contact pressure. On the other hand, those values during the seizure stage were calculated by introducing the coefficient of seizure, which depended on the seizure temperature. The relationship between the seizure temperature and the relative speed at the weld interface in the seizure stage was determined using the experimental results. In addition, the contact pressure and heat generation quantity, which depended on the relative speed of the weld interface, were solved by taking the friction pressure, the relative speed and the yield strength of the base material into the computational conditions. The calculated friction torque and weld interface temperatures of a low carbon steel joint were equal to the experimental results when friction pressures were 30 and 90 MPa, friction speed was 27.5 s^{-1}, and weld interface diameter was 12 mm. The calculation results of the initial peak torque and the elapsed time for initial peak torque were also equal to the experimental results under the same conditions. Furthermore, the calculation results of the initial peak torque and the elapsed time for initial peak torque at various friction pressures were equal to the experimental results.

Key words : Friction Welding, Finite Element Method, Friction Torque, Weld Interface Temperature, Wear Stage, Seizure Stage, Initial Peak Torque, Elapsed Time for Initial Peak Torque

1. Introduction

The friction welding is a well-known solid state joining method. As this method is very useful for joining dissimilar materials, it is widely used in the automobile industry and applied to fabricate important parts such as drive shafts, engine valves, and so on. Generally speaking, the welding cycle of the friction welding by the continuous (direct) drive friction welding can be divided into four stages on the basis of the friction torque curve for a similar material joint,[1] as shown in Fig. 1. In the first stage, the friction torque increases from zero. That

*Received 14 Sep., 2009 (No. 09-0513)
[DOI: 10.1299/jmmp.4.401]

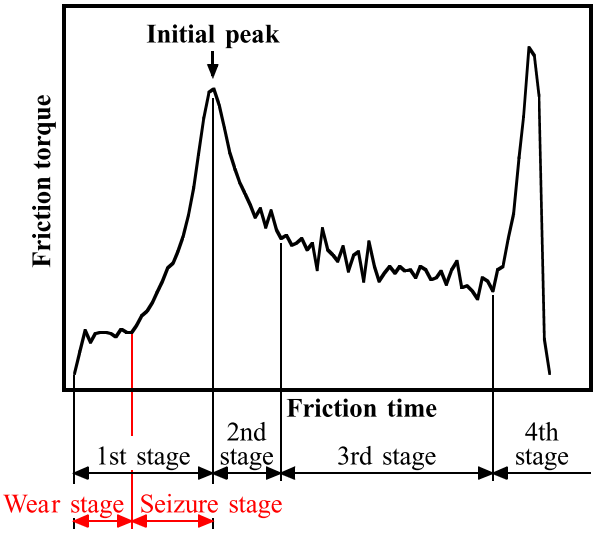

Fig. 1 Definition of stages on the friction torque curve and division of a part in the first stage.

is, the faying (contacting) surfaces of both specimens (workpieces) contact each other, and then the friction torque reaches its initial peak. The second stage is one in which the friction torque reaches a steady (equilibrium) state after the initial peak. The third stage is the steady state. The fourth stage is the forge (upset) stage; in this stage, the friction torque increases when a brake is applied, and then drops to zero when the rotation stops. The sound friction welded joint, of which tensile strength is more than that of the base material, i.e. 100% joint efficiency and fractured in the base metal, can be made through all stages. Also, the friction welding condition for the steel joint was standardized according to Japanese Industrial Standards.[2] However, the selection method of the friction welding condition has not been fully demonstrated, so that each friction welding condition for a material combination is determined by trial and error.

In the previous works,[3]–[9] the authors clarified the joining mechanism during the friction welding process for a similar material joint. Then, the authors showed that the first stage of the friction torque curve can be divided into the wear and seizure stages, which was indicated by red color characters as shown in Fig. 1.[5],[6] In the wear stage, the friction torque is kept almost constant, and the faying surfaces are rubbed against each other. In the seizure stage, the friction torque rapidly increased to the initial peak because joining and separating repeatedly occur at the weld interface. Moreover, the authors showed that the friction welded joints of several steels had 100% joint efficiency using only the first phase (up to the initial peak) of the friction process without increasing forge pressure.[5],[6],[10]–[12] That is, it is considered that the initial peak torque and the elapsed time for initial peak torque become the standard for the selection guideline of the friction welding condition. On the other hand, the authors also proposed that the initial peak torque can be easily calculated by the relationship between the seizure temperature at the weld interface and the yield strength of the base material.[13] However, it is necessary to simulate the initial peak torque and the elapsed time for initial peak torque for various materials because it is expected that this result will be widely applied to the various dissimilar joints. The simulation method for the friction welding is necessary for simulation of the various dissimilar joints for the selection guideline of the friction welding condition, although many researchers have also reported the simulation of friction welding by the finite element method (FEM).[14]–[25] In particular, it is very important to estimate the initial peak torque to know the requirement performance of a friction welding machine in practical use before joining.

Based on the above background, the authors have been simulating the friction torque and the weld interface temperature during the friction process of friction welding. The present

paper focuses on the analysis method of the friction torque and weld interface temperature for steel friction welding. The authors show that the calculation results of the initial peak torque, the elapsed time for initial peak torque and the weld interface temperature were equal to the experimental results of the low carbon steel joint.

2. Joining mechanism of first stage during friction process

Based on the results described in the previous works,[3]–[9] the authors clarified the joining mechanism of the first stage during the friction process for a steel joint. Figure 2 shows the schematic illustration of the joining mechanism model at the first stage during the friction process. In Fig. 2, the illustration on the left side shows low friction pressure, and that on the right side shows high friction pressure. To simplify the joining mechanism, the weld interface is shown by the grouping of concentric circles, shown on the right of the illustrations in Figs. 2a or 2b. Furthermore, the illustrations for (i), (ii), and (iii) are the same in Figs. 2a and 2b. At first, both weld faying surfaces of the base materials contacted each other, and then, both weld faying surfaces were rubbed against each other, which indicated as illustration (i). In this connection, the temperature at the peripheral region of the weld interface was higher than that of the central one because the heat generation depended on the difference of the relative speed at the weld interface. Therefore, the peripheral region was expanded, and the inside regions of the weld interface did not contact, as shown in illustration (ii). Hence, the peripheral region was worn and a fresh surface was created, as indicated in illustration (iii). When the

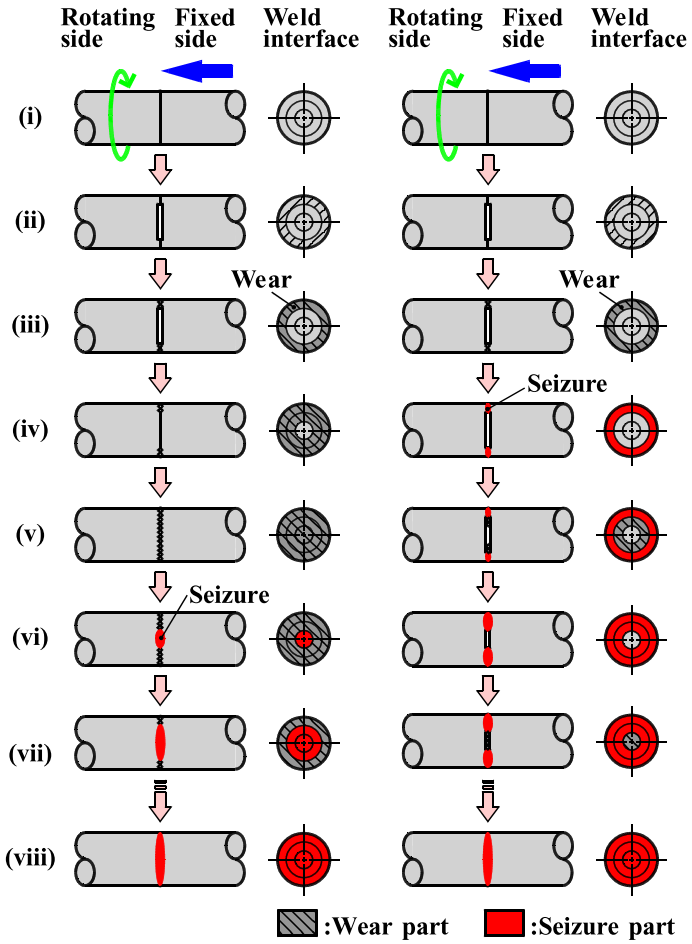

(a) Low friction pressure (b) High friction pressure

Fig. 2 Schematic illustration of the joining mechanism model at the first stage during the friction process; (a) Low friction pressure, (b) High friction pressure.

base materials are welded under low friction pressure such as 30 MPa as shown in Fig. 2a, the yield strength at the peripheral region was decreased, and then the inside regions of the weld interface were rubbed against each other, as indicated in Fig. 2a-(iv). The wear and a fresh surface were repeatedly created from the peripheral region towards the central region, and then the entire weld interface was worn, as shown in Fig. 2a-(v). At this time, the friction torque was kept almost constant, as indicated by the wear stage shown in Fig. 1. The initial seizure and joining began in the central region where the relative speed at the weld interfaces was low because the temperature of the fresh surface was high enough to generate seizure when the friction pressure was low, as shown in Fig. 2a-(vi). Then, the seizure region, i.e. joined region, was extended from the central region towards the peripheral region, as shown in Fig. 2a-(vii). At this time, the friction torque also rapidly increased, which was indicated by the seizure stage shown in Fig. 1. The seizure and joining were repeatedly created from the central region towards the peripheral region, and then the entire weld interface had seizure, as shown in Fig. 2a-(viii). After that, the friction torque reached the initial peak when the entire weld interface had seizure. On the other hand, when the base materials are welded with high friction pressure such as 90 MPa as shown in Fig. 2b, the process from illustrations (i) to (iii) was the same as the case of low friction pressure. The initial seizure and joining began in the peripheral region where the relative speed at the weld interfaces was high because the temperature of the fresh surface was high enough to generate seizure when the friction pressure was high, as shown in Fig. 2b-(iv). Then, the inside regions of the weld interface were rubbed against each other, as shown in Fig. 2b-(v). The wear and seizure were repeatedly created from the peripheral region towards the central region which was indicated as illustrations from (iii) to (vii) in Fig. 2b, and then the entire weld interface had seizure, as shown in Fig. 2b-(viii). As a result, the friction torque also rapidly increased, and then it reached the initial peak when the entire weld interface had seizure. That is, the friction torque did not have the wear stage when the friction pressure was high. It is considered that the friction welding of similar materials could be carried out with the above mechanism.

3. Simulation model

According to above section, the joining phenomena during the friction process of friction welding are very complicated. In the simulation, it is desirable that the actual joining phenomena can be faithfully reproduced. However, it is anticipated that the calculation process is very

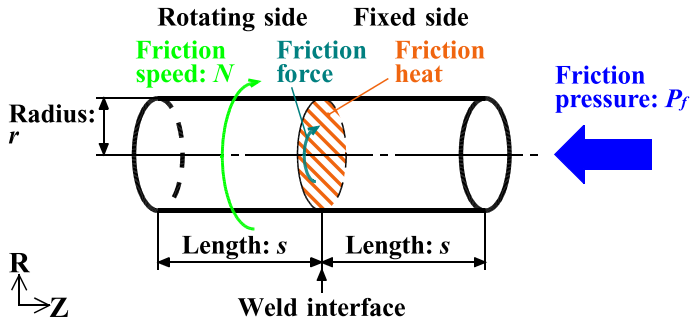

Fig. 3 Schematic illustration of the friction welding model.

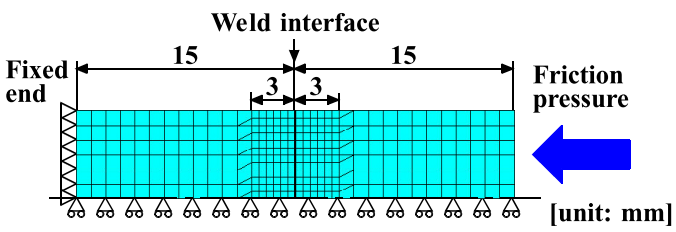

Fig. 4 Schematic illustration of the calculation model.

complicated. To implement calculation easily, the generate flush from the weld interface and the axial shortening (burn-off) of the joint during the friction process were not considered, because the quantity of those were small when the friction torque reached the initial peak. Hence, a simple model of friction welding was used in this study. Figure 3 shows a schematic illustration of the friction welding model. Two round bars with a radius of r and a length of s are contacted at the weld interface with a friction pressure of P_f and a friction speed of N. The friction heat is instantaneously generated at the weld interface, and that heat is simultaneously conducted to the radius and the longitudinal directions. In actual calculation, these above conditions were applied to the non-steady two-dimensional heat transfer analysis. Figure 4 shows the schematic illustration of the calculation model. The calculation model had an axisymmetric body, and a quadrilateral isoparametric element with eight nodes was used. The mesh size was 0.5 × 0.5 mm when the distance in the longitudinal direction was from 0 (the weld interface) to 3.0 mm, and that was 1.0 × 1.0 mm from 3.0 to 15.0 mm. The analysis of the friction torque and the weld interface temperature were carried out by the commercially FEM code ANSYS.

4. Computation method

4.1. Computational algorithm

Figure 5 shows the flowchart of the calculation. The algorithm of the calculation of the friction torque and the weld interface temperature was carried out, and that corresponded with Fig. 5 as follows.

Step 1: The mechanical and thermal properties of the material used and the friction welding conditions are input.

Step 2: The contact pressure and the weld interface temperature of each element are calculated at the time of t. Incidentally, the initial contact pressure is the same as the friction pressure which set. In addition, the initial temperature is room temperature, i.e. 25 °C.

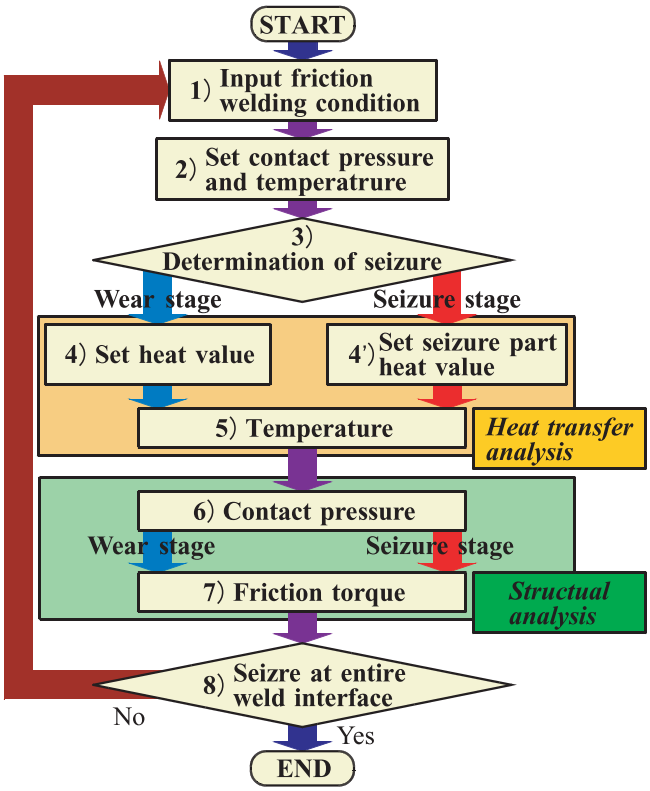

Fig. 5 Flowchart of the calculation.

Step 3: The seizure temperature at the weld interface is determined from the relationship between the contact pressure and the relative speed, and that at the weld interface of each element is calculated from the friction speed that was set. If the weld interface temperature at each element is lower than the seizure temperature, the calculation goes to the next step 4 because the weld interface is in the wear stage. On the other hand, if the weld interface temperature at each element is higher than the seizure temperature, the calculation is going to the next step 4' because the weld interface is in the seizure stage.

Step 4: The heat value is solved with the coefficient of friction, contact pressure, and relative speed, which is indicated as equation (1).

Step 4': The heat value is solved with the coefficient of seizure, contact pressure, and relative speed, which is indicated as equation (2).

$$Q = \mu P_c A v \tag{1}$$

$$Q = \lambda P_c A v \tag{2}$$

In these equations, Q is the heat value [W], μ is the coefficient of friction, λ is the coefficient of seizure, P_c is the contact pressure [Pa], A is an area [mm^2], and v is the relative speed [m/s]. In this connection, the contact pressure and the heat generation quantity are solved by taking the friction pressure, relative speed and yield strength of the base material into the conditions.

Step 5: The weld interface temperature of each element at the time of $t + \Delta t$ is determined by the heat value that was calculated at step 4 or 4'.

Step 6: The contact pressure at the weld interface of each element at the time of $t + \Delta t$ is determined, and that value also includes the thermal stress at the same time.

Step 7: The friction torque of each element at the time of $t + \Delta t$ is solved by using the contact pressure. The friction torque at the wear stage is calculated using the coefficient of friction, which is indicated as equation (3). Similarly, the friction torque at the seizure stage is calculated using the coefficient of seizure, which is indicated as equation (4).

$$T = \mu P_c A r \tag{3}$$

$$T = \lambda P_c A r \tag{4}$$

In these equations, T is the torque [Nm] and r is the radius [m].

Step 8: The heat value at the weld interface and the friction torque at each element are repeatedly calculated from steps 1 to 8 by using the temperature and the contact pressure, which are solved at steps 5 and 6. Then, when the entire weld interface will be obtained the seizure region, the calculation is finished.

4.2. Calculation of seizure temperature

In the previous work,[9] the initial seizure at the friction surface was generated in the following conditions; the temperature and the loaded pressure were 150 °C or over and 30 MPa, and 50 °C or over and 90 MPa, respectively. Moreover, it was clarified that the seizure temperature increased with increasing relative speed at the weld interface.[9] Based on these results, the seizure temperature was experimentally derived, as indicated in equations (5a) and (5b).

$$\theta = 1200.00 - 1.67 P_c + 2717.86 v \qquad (0 < v \leq 0.14) \tag{5a}$$

$$\theta = 566.50 - 1.67 P_c + 100.00 v \qquad (0.14 \leq v) \tag{5b}$$

In these equations, θ is the seizure temperature [°C].

4.3. Calculation of coefficient of seizure

It was clarified that the friction torque reached the initial peak after when the entire weld interface had seizure, regardless of the friction pressure.[5),6),10)−12)] Based on these results, the coefficient of seizure was defined by the relationship between the friction pressure and the fracture strength of the seizure portion at the weld interface, and that was determined using the initial peak torque in the previous experiments,[5)−7)] as indicated in equation (6).

$$T_{it} = \lambda P_f \int_0^R 2\pi r \cdot r dr = \frac{2\pi\lambda P_f}{3} R^3 \tag{6}$$

In these equations, T_{it} is the initial peak torque [Nm] and P_f is the friction pressure [Pa]. Hence, the coefficient of seizure was obtained from the following equation by substituting the value of the initial peak torque at friction pressures of 30 and 90 MPa into equation (6).

$$\lambda(v, T_e, P_f) = 0.45 + \left(\lambda_{30}(v, T_e) - 0.45\right)\left(\frac{\lambda_{90}(v, T_e) - 0.45}{\lambda_{30}(v, T_e) - 0.45}\right)^{\frac{P_f}{60} - \frac{1}{2}} \tag{7}$$

$$\lambda_{30}(v, T_e) = 1.30\exp(-2.50v) + 1.48\log T_e - 2.08$$

$$\lambda_{90}(v, T_e) = 1.30\exp(-2.50v) + 0.91\log T_e - 1.56$$

In these equations, T_e is the temperature [°C], λ_{30} and λ_{90} are the coefficients. Incidentally, those equations were carried out for the calculation as the subprogram in ANSYS.[26)] Also, the thermal boundary conditions of the specimens were not considered, because those were not effective for the calculated results.

5. Results and Discussion

5.1. Temperature and friction torque during friction process

Tables 1 and 2 show the mechanical and thermal properties of low carbon steel.[13),27)] The mechanical and thermal properties of low carbon steel were used and those values were dependent on the temperature in this study. The value at each temperature were used by linear

Table 1 Mechanical properties low carbon steel for calculation.[13)]

Temperature, ℃	20	50	70	93	150	200	255	300
Young's modulus, GPa	192			191	189	186	182	
Yield stress, MPa	318		341			265		
Shear stress, MPa		317			342	358	362	352
Temperature, ℃	315	371	380	400	427	482	500	538
Young's modulus, GPa	177	171			162	127		106
Yield stress, MPa			224					
Shear stress, MPa				176			110	
Temperature, ℃	593	600	750	800	1000	1200	1400	1500
Young's modulus, GPa	89				5	0.6		
Yield stress, MPa			38				1.1	
Shear stress, MPa		100		127	80	50		1

Table 2 Thermal properties of low carbon steel for calculation.[27)]

Temperature, ℃	27	100	200	400	600	800	1000	1200
Thermal conductivity, W/mK	51.6	51.1	49.0	42.7	35.6	26.0	27.2	29.7
Specific heat, J/kgK	473	486	520	599	749	950	644	661
Coefficient of liner expansion, $℃^{-1}(\times 10^{-6})$	11.80	12.18	12.66	13.47	14.41	12.64	13.37	

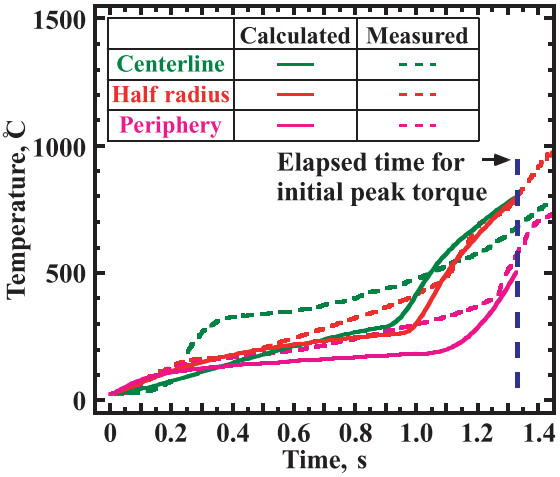

(a) Friction pressure of 30 MPa

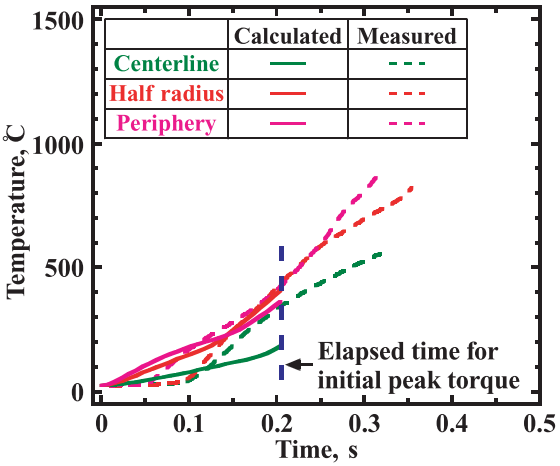

(b) Friction pressure of 90 MPa

Fig. 6 Calculation results of temperatures at centerline, half radius, and periphery portions, with measured temperatures at those portions; friction pressure of (a) 30 MPa and (b) 90 MPa.

interpolation from Tables 1 and 2. The calculation was carried out by using the following condition: weld interface diameter of 12 mm (its radius was 6.0 mm), friction pressures of 30 and 90 MPa, and friction speed of 27.5 s^{-1} (1650 rpm). Figure 6 shows the calculation results of the temperatures at the centerline, half radius, and periphery portions. Figure 6 also includes the measured temperatures of those portions. The low carbon steel was welded by a direct drive friction welding machine, and the temperatures were measured at the centerline, half radius, and periphery portions of the 1.0 mm longitudinal direction from the weld faying surface by mineral insulated thermocouples with a chromel-alumel. The friction torque was also measured simultaneously with the measuring temperature. The details of the specimen shape for the measuring temperature changes, the joining method, and the measurement method of the friction torque and temperature have been described in the previous reports.[28]–[30] The calculated temperatures at the centerline, half radius, and periphery portions were also carried out under the same conditions of the experiment. When friction pressure was 30 MPa as shown in Fig. 6a, the calculated centerline temperature was smoothly increased at a time of about 0.2 s, although the measured centerline temperature was rapidly increased at the same friction time. However, the calculated centerline temperature was equal to the measured centerline temperature when the friction torque reached the initial peak, i.e. about 1.3 s. In addition, the calculated half radius and periphery temperatures were similar to that of the measured temperatures. On the other hand, when friction pressure was 90 MPa as shown in Fig. 6a,

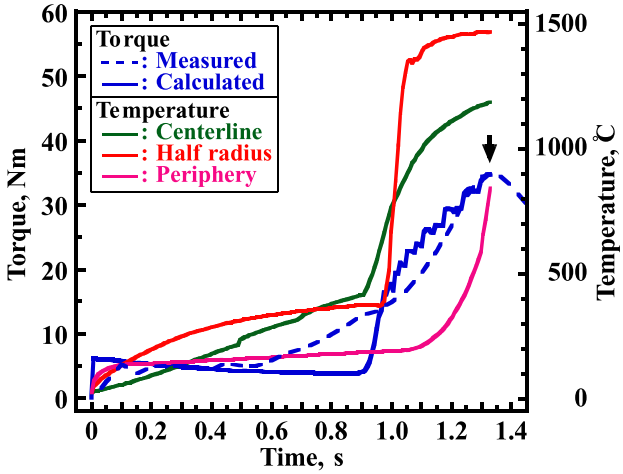

(a) Friction pressure of 30 MPa

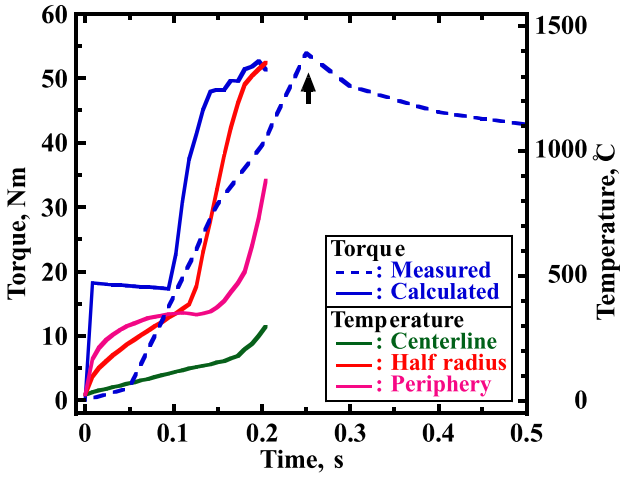

(b) Friction pressure of 90 MPa

Fig. 7 Calculated friction torque and weld interface temperatures at centerline, half radius, and periphery portions, with measured friction torque; friction pressure of (a) 30 MPa and (b) 90 MPa.

the calculated temperatures at those portions were also similar to the measured temperatures. That is, the calculated temperatures were equal to the measured temperatures under friction pressures of 30 and 90 MPa. Incidentally, the temperature at the periphery portion was not measured after a friction time of about 0.2 s because the thermocouples were broken by the flash, which was exhausted. Figure 7 shows the calculated friction torque and the weld interface temperatures at the centerline, half radius, and periphery portions. Figure 7 also includes the measured friction torque. When friction pressure was 30 MPa, the calculated weld interface temperature at the centerline portion was rapidly increased at a time of about 0.9 s, which was shown in Fig. 7a. The central portion of the weld interface had seizure at a friction time of about 0.7 s in the experiment. That is, the rapid increase of the temperature in the calculation was evidence that this portion had seizure. Then, the rapid increase of the temperature at the weld interface in the calculation at the half radius and periphery portions was obtained at times of about 0.95 and 1.2 s, respectively. That is, the seizure was also obtained toward the periphery portions from the central portions in the calculation. Moreover, the calculated friction torque was similar to the measured friction torque, and those of the initial peak torque and the elapsed time for the initial peak torque were equal to the experimental result, which was indicated by the arrow in Fig. 7a. On the other hand, when friction pressure was 90 MPa, the calculated friction torque was similar to the measured friction torque, although the

elapsed time for the initial peak torque by the calculation was slightly shorter than that of the experimental result indicated by the arrow in Fig. 7b. That is, the calculated friction torque was also equal to the experimental results under friction pressures of 30 and 90 MPa.

5.2. Calculation of initial peak and elapsed time for initial peak torque at various friction pressures

Figure 8 shows the calculation results of the initial peak torque and the elapsed time for the initial peak torque at various friction pressures. Figure 8 also shows the measured results for reference.[3)−9),12)] The calculated initial peak torque increased with increasing friction pressure, and it kept almost constant when friction pressure was 100 MPa or over, as shown in Fig. 8a. In addition, the calculated elapsed time for the initial peak torque decreased with increasing of friction pressure, as shown in Fig. 8b. That is, the calculation results of the initial peak torque and the elapsed time for the initial peak torque at various friction pressures were equal to the experimental results, although those values slightly differed at friction pressure of 150 MPa. Incidentally, friction pressure such as 150 MPa or over was not the practical condition because the central region of the weld interface of the joint was not welded and the joint did not have the base material fracture.[12)] Although further investigation is necessary to elucidate the detailed simulation method to apply to the various materials, the friction torque

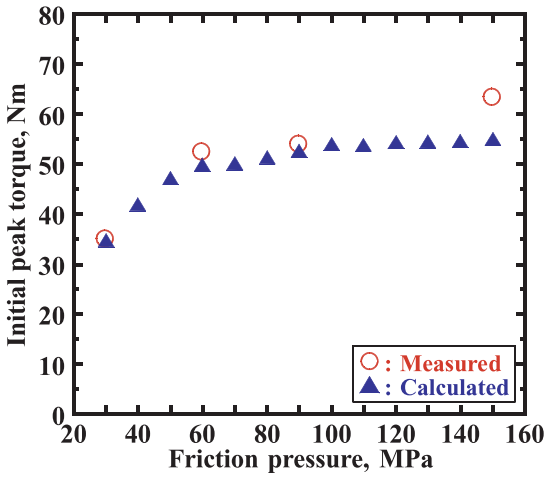

(a) Initial peak torque

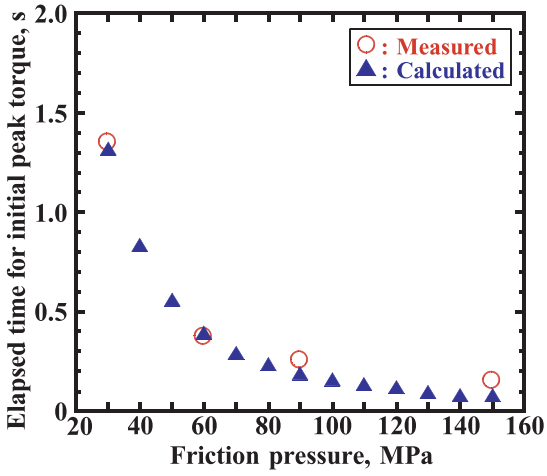

(b) Elapsed time for initial peak torque

Fig. 8 Calculationd results of initial peak torque and elapsed time for initial peak torque at various friction pressures corresponding to experimental results; (a) Initial peak torque, (b) Elapsed time for initial peak torque.

and the weld interface temperature could be simulated by using the seizure properties of the base material under the practical condition.

6. Conclusions

This report described an analysis method for the friction torque and weld interface temperature during the friction process of steel friction welding. The non-steady two-dimensional heat transfer analysis for the friction process was carried out by calculation with FEM code ANSYS. Moreover, the joining mechanism model of the friction welding for the wear and seizure stages was constructed from experimental results. The following conclusions are provided.

(1) The contact pressure, heat generation quantity, and friction torque during the wear stage were calculated using the coefficient of friction, which was assumed as the constant value in the actual analysis. Those values during the seizure stage were calculated by using the coefficient of seizure which depended on the seizure temperature. In addition, the contact pressure and thermal stress at the weld interface in the wear stage, and the relationship between the seizure temperature and the relative speed at the weld interface in the seizure stage were considered. The contact pressure and heat generation quantity, which depended on the relative speed at the weld interface, were solved by taking the friction pressure, relative speed and yield strength of the base material into the computational conditions.

(2) The calculation results of the temperatures at the centerline, half radius, and periphery portions of the 1.0 mm longitudinal direction from the weld faying surface were equal to the experimental temperatures when friction pressures were 30 and 90 MPa, friction speed was 27.5 s^{-1}, and weld interface diameter was 12 mm for the low carbon steel joint. In addition, the calculated friction torque was also equal to the experimental results under the same conditions.

(3) The calculation results of the initial peak torque and the elapsed time for initial peak torque at various friction pressures were equal to the experimental results, although those values slightly differed at friction pressure of 150 MPa.

Acknowledgements

This research was partially supported by the Ministry of Education, Culture Sports, Science and Technology, Grant-in-Aid for Young Scientists (B), 20760496, 2008. We wish to thank the staff members of the Machine and Workshop Engineering at the Graduate School of Engineering, University of Hyogo.

References

(1) Hasui, A. and Fukushima, S., On the Torque in Friction Welding, *Journal of the Japan Welding Society*, Vol. 44, No. 12 (1975), pp. 1005-1010. (in Japanese)

(2) Japanese Industrial Standards Committee, JIS Z3607 Recommended practice for friction welding of carbon steel, (1994), (in Japanese)

(3) Kimura, M., Mioh, H., Kusaka, M., Seo, K., and Fuji, A., Observation of the Joining Phenomena in First Phase of Friction Welding, *Quarterly Journal of the Japan Welding Society*, Vol. 20, No. 3 (2002), pp. 425-431. (in Japanese)

(4) Kimura, M., Kusaka, M., Seo, K., and Fuji, A., Effect of Various Conditions on Friction Torque in First Phase of Friction Welding, *Quarterly Journal of the Japan Welding Society*, Vol. 20, No. 3 (2002), pp. 432-438. (in Japanese)

(5) Kimura, M., Kusaka, M., Seo, K., and Fuji, A., Observation of Joining Phenomena in Friction Stage and Improving Friction Welding Method, *JSME International Journal (Series A)*, Vol. 46, No. 3 (2003), pp. 384-390.

(6) Kimura, M., Kusaka, M., Seo, K., and Fuji, A., Relationship between the Friction Time, Friction Torque, and Joint Properties of Friction Welding for the Low Heat Input Friction Welding Method, *Quarterly Journal of the Japan Welding Society*, Vol. 20, No. 4 (2002), pp. 559-565. (in Japanese)

(7) Kimura, M., Ohtsuka, Y., An, G. B., Kusaka, M., Seo, K., and Fuji, A., Effect of Friction Speed on Initial Seizure Portion on Welded Interface, *Quarterly Journal of the Japan Welding Society*, Vol. 21, No. 4 (2003), pp. 615-622. (in Japanese)
(8) Kimura, M., Kusaka, M., Seo, K., and Fuji, A., Effect of Inner Diameter on Friction Torque in Friction Welding of Pipes, *Quarterly Journal of the Japan Welding Society*, Vol. 22, No. 2 (2004), pp. 233-239. (in Japanese)
(9) Kimura, M., An, G. B., Kusaka, M., Seo, K., and Fuji, A., An Experimental Study of Seizure Phenomena at Welded Interface of Steel Friction Weld, *Quarterly Journal of the Japan Welding Society*, Vol. 23, No. 3 (2005), pp. 460-468. (in Japanese)
(10) Kimura, M., Kusaka, M., Seo, K., and Fuji, A., Improving Joint Properties of Friction Welded Joint of High Tensile Steel, *JSME International Journal (Series A)*, Vol. 48, No. 4 (2005), pp. 399-405.
(11) Kimura, M., Kusaka, M., Seo, K., and Muramatsu, Y., Properties and improvement of super fine grained steel friction welded joint, *Science and Technology of Welding and Joining*, Vol. 11, No. 4 (2006), pp. 448-454.
(12) Kimura, M., Ohtsuka, Y., Kusaka, M., Seo, K., and Fuji, A., Effect of Friction Time and Friction Pressure on Tensile Strength of Welded Joint for Medium and High Carbon Steels by Low Heat Input Friction Welding Method, *Quarterly Journal of the Japan Welding Society*, Vol. 23, No. 4 (2005), pp. 577-586. (in Japanese)
(13) Kimura, M., Yoshioka, K., Kusaka, M., Seo, K., and Fuji, A., Simulation of Friction Torque in First Phase of Friction Welding, *Quarterly Journal of the Japan Welding Society*, Vol. 20, No. 4 (2002), pp. 546-551. (in Japanese)
(14) Suga, Y., Ozawa, J., Miyakawa, S., and Ogawa, K., Estimation of Temperature Distribution in Friction Weld of Carbon Steel by Finite Element Method, *Journal of the Japan Friction Welding Association*, Vol. 5, No. 2 (1995), pp. 43-50. (in Japanese)
(15) Moal, A. and Massoni, E., FINITE ELEMENT SIMULATION OF THE INERTIA WELDING OF TWO SIMILAR PARTS, *Engineering Computations*, Vol. 12, Issue 6 (1995), pp. 497-512.
(16) Sahin, A. Z.,Yibas, B. S., Ahmed, M., and Nickel, J., Analysis of the friction welding process in relation to the welding of copper and steel bars, *Journal of Materials Processing Technology*, Vol. 82 (1998), pp. 127-136.
(17) Ikeshoji, T., Demura, N., Suzumura, A. and Yamazaki, T., Heat Analysis in Friction Welding Joint of Stainless Steel, *Proceedings of the 12th Materials and Processing Conference*, No. 04-15 (2004-11), pp. 311-312. (in Japanese)
(18) Fu, L., Duan, L. Y., and Du, S. G., Numerical Simulation of Inertia Friction Welding Process by Finite element Method, *Welding Journal*, Vol. 82 (2003), pp. 65s-70s.
(19) Sahin, M., Simulation of friction welding using a developed computer program, *Journal of Materials Processing Technology*, Vol. 153-154 (2004), pp. 1011-1018.
(20) Isshiki, Y., Yamaguchi, H., Kawai, G., and Ogawa, K., Numerical Analysis of Temperature Distribution in Friction Welding of Carbon steel, *Journal of High Temperature Society*, Vol. 31, No. 4 (2005), pp. 225-231. (in Japanese)
(21) Kahveci, K., Can, Y., and Cihan, A., HEAT TRANSFER IN CONTINUOUS-DRIVE FRICTION WELDING OF DIFFERENT DIAMETERS, *Numerical Heat Transfer Part A*, Vol. 48 (2005), pp. 1035-1050.
(22) Nguyen, T. C. and Weckman, D. C., A Thermal and Microstructure Evolution Model of Direct-Drive Friction Welding of Plain Carbon Steel, *Metallurgical and Materials Transactions B*, Vol. 37B, No. 4 (2006), pp. 275-292.
(23) Qinghua, L., Fuguo, L., Miaoquan, L., Qiong, W., and Fu, L., Finite element Simulation of Deformation Behavior in Friction Welding of Al-Cu-Mg Alloy, *Journal of Materials Engineering and Performance*, Vol. 15, No. 6 (2006), pp. 627-631.
(24) Ohkubo, Y., Iwamura, S., and Hatta, H., Thermal Analysis on Friction welding of Carbon steel Tube and AA5154 Aluminum Tube, *Sumitomo Light Metal Technical Reports*,

Vol. 48, No. 1 (2007), pp. 27-32. (in Japanese)

(25) Rao, A. V., Kumar, R. K., Mohandas, T., and Reddy, G. M., SOME CRITICAL ISSUES IN THE FINITE ELEMENT ANALYSIS OF FRICTION WELDING, *Metals Materials And Processes*, Vol. 19, No. 1-4 (2007), pp. 127-136.

(26) ANSYS, Inc., *ANSYS Seminar Note: APDL Guide Seminar*, (2004), Cybernet Systems Co. Ltd. (in Japanese)

(27) Japan Society of Thermophysical Properties ed., *Thermophysical Properties Handbook*, (2008), pp.210, Yokendo. (in Japanese)

(28) Kimura, M., Kusaka, M., Kaizu, K., and Fuji, A., Effect of Friction Welding Condition on Joining Phenomena and Tensile Strength of Friction Welded joint between Pure Copper and Low Carbon Steel, *Journal of Solid mechanics and Materials Engineering*, Vol. 3, No. 2 (2009), pp. 189-198.

(29) Kimura, M., Ishii, H., Kusaka, M., Kaizu, K., and Fuji, A., Joining phenomena and joint strength of friction welded joint between pure aluminium and low carbon steel, *Science and Technology of Welding and Joining*, Vol. 14, No. 5 (2009), pp. 388-395.

(30) Kimura, M., Kasuya, K., Kusaka, M., Kaizu, K., and Fuji, A., Effect of friction welding condition on joining phenomena and joint strength of friction welded joint between brass and low carbon steel, *Science and Technology of Welding and Joining*, Vol. 14, No. 5 (2009), pp. 404-412.